DOI: 10.1002/ange.201300755

Silicon Etching

The Stoichiometry of Electroless Silicon Etching in Solutions of V_2O_5 and HF

Kurt W. Kolasinski* and William B. Barclay

The etching of silicon is of fundamental importance in the manufacture of semiconductor devices, in the fabrication of microelectromechanical systems, and increasingly in materials chemistry.[1] The wet-chemical etching of Si in HNO_3/HF, an electroless electrochemical process, is an essential step in the manufacture of solar cells.[2] When performed under conditions for the formation of porous silicon (por-Si), the process is known as stain etching. It can be initiated by a variety of more suitable oxidizing agents[3] and can be used for the low-cost production of nanocrystalline por-Si powder[4] or Si nanocrystals.[5] Nonetheless, we still lack the most basic chemical understanding of this reaction: the reaction stoichiometry is unknown. Herein we conclusively report the reaction stoichiometry and interpret it fundamentally in terms of Marcus theory of electron transfer and the Gerischer model of Si etching.

Silicon is etched anodically in fluoride solutions to form porous silicon according to the Gerischer mechanism.[6] The current-doubling pathway shown in Scheme 1 is the dominant reaction pathway. It has a valence of 2 resulting from hole injection into the valence band of Si in step 1 and electron injection into the conduction band in step 3. This process can be broken down into two electrochemical reactions. Reaction (1) describes etching, and reaction (2) is the counter reaction that occurs at a Pt electrode:

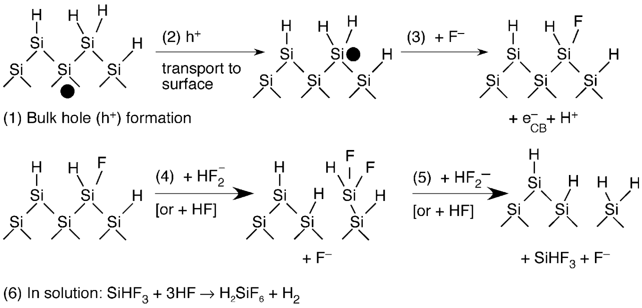

Scheme 1. Current-doubling pathway for silicon etching.

$$Si(s) + 2\,HF + 2\,HF_2^- + h_{VB}^+ \rightarrow H_2SiF_6 + H_2(g) + e_{CB}^- \qquad (1)$$

$$H^+ + e_{CB}^- \rightarrow 1/2\,H_2(g) \qquad (2)$$

In these equations, the aqueous-phase notation is omitted for brevity. The overall stoichiometry is $h_{VB}^+/Si = 1{:}1$ and $H_2/Si = 3{:}2$. That is, one hole is injected into the valence band and 1.5 mol of H_2 are produced for each mole of Si atoms etched. Note that 1 mol of H_2 comes from a surface reaction, and 0.5 mol comes from a solution-phase reaction.

It is commonly assumed[7] that the sole role of the oxidant in electroless etching is to inject the holes required in Equation (1). Accordingly, the stoichiometry of stain etching should be exactly the same as for anodic etching. The stoichiometry of the $HNO_3 + HF$ system is extremely complex because of the nature of the oxidant and the formation of numerous intermediate species. The interpretation of reaction data is far from straightforward, although detailed experiments have greatly improved our understanding of etching in the electropolishing regime.[2]

The discovery of stain etching with V_2O_5 as the oxidant[8] provides a unique opportunity to study the stoichiometry of stain etching. The half-reaction that injects a hole into (equivalently, removes an electron from) the Si valence band is:

$$VO_2^+ + 2\,H^+ + e_{CB}^- \rightarrow VO^{2+} + H_2O. \qquad (3)$$

No gas is generated, and one hole is injected for each V^V atom that is reduced. As we demonstrate herein, both the V^V oxidation state, as in VO_2^+, and V^{IV}, as in VO^{2+}, are quantifiable by UV/Vis absorption spectroscopy, and the measurement of pressure changes under isothermal conditions provides a direct measurement of the amount of H_2 generated during etching.

Figure 1 displays the absorption spectra recorded during the etching of single crystal chunks of Si in a solution of V_2O_5 (0.023 M) in HF/H_2O (1:3) at 273 K. We confirmed the linear relationship between absorbance and concentration by Beer–Lambert analysis for both VO_2^+ and VO^{2+} and used this analysis to demonstrate the quantitative conversion of VO_2^+ into VO^{2+} within the accuracy of absorption spectroscopy performed at high and variable ionic strengths (Figure 2).

It has long been assumed but never proven that hole injection is the rate-limiting step for stain etching.[3,7a] We performed etching at a low VO_2^+ concentration (ca. 0.02 M) and a virtually constant fluoride concentration (ca. 7 M). Our infrared spectroscopic and kinetics data on the etching of single crystals[9] revealed that after a pore-nucleation phase, a constant surface area at the bottom of a fixed number of pores is responsible for etching. Therefore, the limiting reagent is VO_2^+, and we expected the reaction to follow pseudo-first-order kinetics with an apparent rate constant k_V as a function of etch time, t, for both the decrease in the VO_2^+

---

[*] Prof. K. W. Kolasinski, W. B. Barclay
Department of Chemistry, West Chester University
West Chester, PA 19383 (USA)
E-mail: k.w.kolasinski@wcupa.edu
Homepage: http://courses.wcupa.edu/kkolasinski/surfacescience/

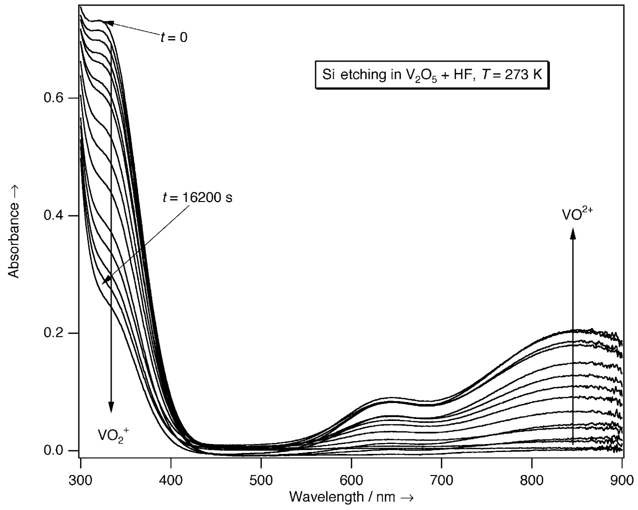

Figure 1. UV/Vis absorption spectra as a function of etch time.

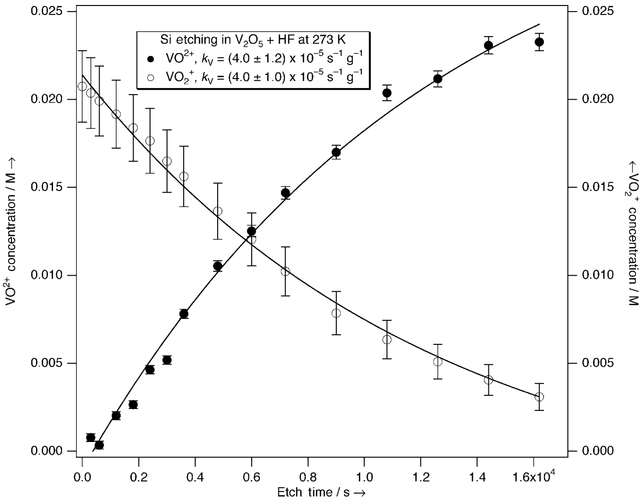

Figure 2. Fits (solid lines) confirm that the conversion of VO_2^+ into VO^{2+} during Si etching followed pseudo-first-order kinetics. The concentrations of these two species were determined by UV/Vis spectroscopy as a function of etch time (from the data in Figure 1).

concentration and the increase in the VO^{2+} concentration according to the following equations:

$$[VO_2^+] = [VO_2^+]_0 \exp(-k_v t) \tag{4}$$

$$[VO^{2+}] = [VO^{2+}]_\infty (1-\exp(-k_v t)). \tag{5}$$

The fits to Equations (4) and (5) shown in Figure 2, normalized with respect to the mass of the Si used, confirm the pseudo-first-order behavior for the decay of VO_2^+ and the appearance of VO^{2+}. Thus, the reduction of VO_2^+ to VO^{2+} is not followed by any further electrochemistry. The etch rate is orders of magnitude below the diffusion-limited rate. Hole injection into H-terminated Si must be the rate-determining step. Subsequent reactions in the etch mechanism (including completion of the dioxovanadium(V) half-reaction) are fast and kinetically irrelevant. These results provide the first direct evidence that the hole-injection step is indeed the rate-determining step in stain etching.

We confirmed the reproducibility and consistency of the data by measuring the rate constant as a function of temperature. The results are presented in Figure 3 as an Arrhenius plot, with 95% confidence-limit error bars, and are well-described by Arrhenius behavior. The activation energy determined from the data is $E_a = 30 \pm 5$ kJ mol^{-1}.

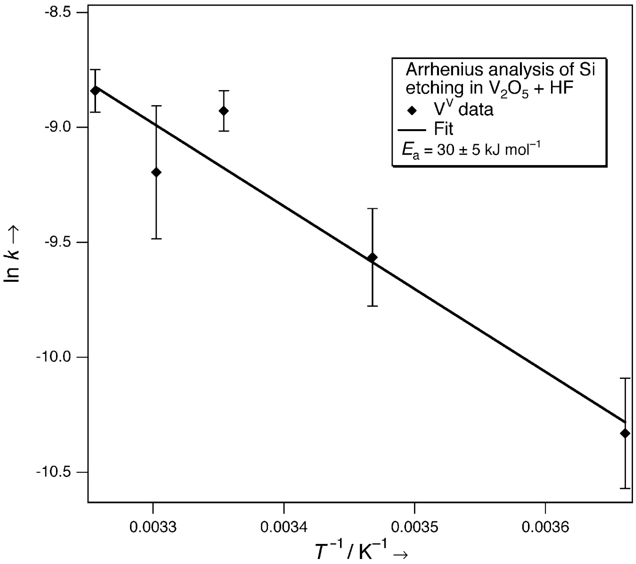

Figure 3. Arrhenius analysis of the etch rate constant determined over the temperature range 273–307 K.

Recently, we performed calculations to quantitatively compare the etch rates of various stain etchants with the predictions of Marcus theory for the rate of hole injection.[3] These calculations demonstrated that Marcus theory provides a good description of the etch rate for the reaction of V_2O_5 and HF with Si(100) substrates. It was determined that the rate constant is given by:

$$k = A \exp(-E_a/RT) = A \exp(-\lambda/4k_B T) \tag{6}$$

in which R is the gas constant, λ the reorganization energy, k_B the Boltzmann constant, and A the pre-exponential factor. We reported that $\lambda = 1.27 \pm 0.2$ eV, from which a value of $E_a = 31 \pm 5$ kJ mol^{-1} is predicted; this value is in excellent accord with the data in Figure 3.

By gravimetric analysis of the etched Si, we determined the amount of Si etched in moles. UV/Vis spectroscopy was used to quantify the total amount in moles of VO_2^+ that reacted. We determined the amount of H_2 evolved during etching from pressure changes during etching under isothermal conditions in a vessel of known volume. As confirmed in Figure 4, the evolution of H_2 also follows pseudo-first-order kinetics. From these sets of measurements we were able to determine the VO_2^+/Si and H_2/Si molar ratios. By analogy with anodic etching, we expected VO_2^+/Si = 1:1 and H_2/Si = 1.5:1. However, we found VO_2^+/Si = (1.98 ± 0.13):1 and H_2/Si = (1.01 ± 0.08):1, again with 95% confidence limits.

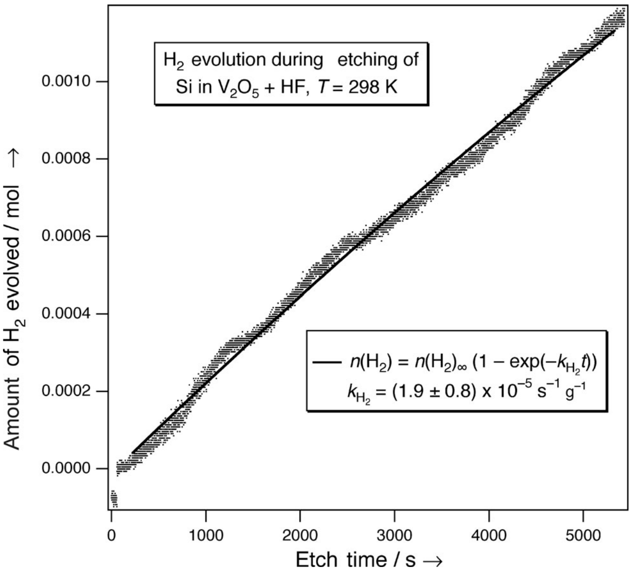

Figure 4. The evolution of H_2 versus etch time, as determined by pressure measurements, confirms the pseudo-first-order kinetics of the process. The curve drawn through the data points is defined by the equation shown.

The simultaneous doubling of the VO_2^+ consumption and 50% reduction in the H_2 evolution is explained by etching according to the following reaction:

$$\mathrm{Si} + 2\,\mathrm{HF} + 2\,\mathrm{HF_2}^- + \mathrm{VO_2}^+ \rightarrow \mathrm{SiF_6}^{2-} + \mathrm{H_2} + \mathrm{VO}^{2+} + \mathrm{H_2O} + \mathrm{e_{CB}}^- \qquad (7)$$

which is accompanied by a charge-balancing counter reaction:

$$\mathrm{VO}^{2+} + 2\,\mathrm{H}^+ + \mathrm{e_{CB}}^- \rightarrow \mathrm{VO}^{2+} + \mathrm{H_2O} \qquad (8)$$

This stoichiometry requires that the true rate constant is equal to the apparent rate constant of H_2 formation and half the apparent rate constant of VO_2^+ consumption (or VO^{2+} formation): $k = k_{H_2} = 1/2k_V$, precisely as determined in our study. This stoichiometry only makes sense if the rate of conduction-band electron transfer to VO_2^+ by reaction (8) greatly exceeds the rate of conduction-band electron transfer to H^+ by reaction (2). VO_2^+ with $E° = 0.91$ V lies approximately 1 eV below the conduction-band edge. H^+ at $E° = 0$ V lies just a few tenths of an electron volt below the conduction-band minimum, E_C.[3,10] According to Marcus theory, the rate of electron transfer is proportional to the probability hop factor, W, which depends on the electrochemical potential of the oxidant, E_{ox}, according to the following equation:

$$W(E_{ox}) = \exp[-((E_C - E_{ox} + \lambda)^2/4\lambda k_B T)] \qquad (9)$$

Thus, conduction-band electron transfer to VO_2^+ is near the optimal value, because $E_C - E_{ox} + \lambda \approx 0.14$ eV. With an estimate of the reorganization energy based only on an outer-sphere contribution calculated from the size of the solvated proton, the rate of electron transfer to H^+ would be roughly 5 orders of magnitude lower if it were described by an outer-sphere process, because $E_C - E_{ox} + \lambda \approx -0.22 - 0 + 1.43 \approx 1.21$ eV. A good hydrogen-recombination catalyst 1) has a d band that straddles the Fermi energy, 2) does not bind H atoms too strongly, and 3) does not present a barrier to H_2 dissociation.[11] Si fails on all of these counts and is a decidedly inferior catalyst. Although it is unlikely that electron transfer to H^+ is well described by an outer-sphere process, it is also unlikely that a more appropriate process involving specific adsorption is as rapid as is electron transfer to VO_2^+ because Si is such a poor catalyst and the E_{ox} value of VO_2^+ is nearly optimal. Therefore, the observed kinetics and stoichiometry are completely consistent with the expectations of Marcus theory.

Our results overturn the conventional wisdom regarding the role of the oxidant in the reaction because the above reasoning is valid for all oxidants known to initiate stain etching. These results also have implications for metal-assisted etching, for which the oxidant that interacts with the metal catalyst deposited on a Si surface has been assumed to play only the role of the hole injector, as was previously assumed for stain etching. Metal-assisted etching[1c] is a rapidly advancing synthetic technique that can lead to ordered arrays of Si nanowires or macropores of interest for their thermoelectric, optoelectronic, lithium-storage, antireflective, sensing, and biocompatible properties, among others.[12] In future studies, we will investigate how the presence of the metal nanoparticle catalyst influences the stoichiometry and valence of the etching reaction.

Experimental Section

Our experimental setup and data analysis have been described in detail elsewhere.[13] Etching was performed on Si(100) 0–100 Ω cm p-type test-grade wafers, Si(111) mechanical-grade n-type wafers (both UniversityWafer), or unpolished single-crystal-reclaimed wafer chunks (Union Carbide). The wafer chunks serve as a nonbuoyant, high-purity sample with a moderate surface area (high relative to that of wafers, low relative to that of a powder). Chunks were sieved to obtain a narrow size distribution (3.35–4.75 mm), and a large enough sample size was used (ca. 2 g) to ensure a constant initial surface area. The silicon was cleaned by ultrasonication first in acetone and then in ethanol, followed by rinsing with water. Exposure of the samples to air after cleaning was minimized. After etching, samples were rinsed with water and ethanol and then dried in a stream of Ar gas. V_2O_5 (Fisher certified grade) and HF (JT Baker 49% analytical grade) were used. Concentrated HF was diluted in a 1:3 ratio with water. $VOSO_4$ (Strem) was used as a source of VO^{2+}(aq) for Beer–Lambert calibration.

Large single crystals of Si(100) and Si(111) etch slowly because of the low surface area. The cleavage of these crystals into a large number of small crystals leads to a high enough reaction rate for the determination of the reaction stoichiometry; however, the etch rate varies greatly from sample to sample, because the etch rate is influenced strongly by defects. This method is not reliable for the determination of kinetic parameters (rate constant, activation energy). Therefore, we used chunks of semiconductor wafers to determine the rate constant and activation energy.

V_2O_5 dissolves in HF to form VO_2^+, which is reduced to VO^{2+} during por-Si formation. The decrease in the concentration of VO_2^+ and the increase in the concentration of VO^{2+} were monitored by UV/Vis spectroscopy on a Cary 300 Bio UV/Vis spectrometer. We used poly(methyl methacrylate) cuvettes for UV/Vis spectroscopy because of the HF/H_2O (1:3) solvent, which limited the detection of wavelengths above 300 nm. At $\lambda = 330$ nm, the molar absorptivity of the VO_2^+ species is $\varepsilon(330\,\text{nm}) = 31.7 \pm 4.6\,\text{M}^{-1}\,\text{cm}^{-1}$. VO^{2+} absorbs at 846 nm with $\varepsilon(846\,\text{nm}) = 8.89 \pm 0.17\,\text{M}^{-1}\,\text{cm}^{-1}$. VO^{2+} also absorbs with $\varepsilon(330\,\text{nm}) = 3.55 \pm 0.04\,\text{M}^{-1}\,\text{cm}^{-1}$.

The pressure and temperature as a function of time were monitored with a MicroLAB 4205 unit interfaced with a computer. Two 750 mL high-density polyethylene (HDPE) Erlenmeyer filter flasks were connected by a short section of Tygon tubing. The reaction and ballast flasks were both stoppered and submerged in a thermostated bath. The ballast flask was connected through its stopper by a thin Teflon tube to a pressure sensor. Mass spectral analysis of the gas phase did not reveal the presence of any gases containing V, Si, or F other than HF. The temperature and pressure were continuously monitored each second for a period of 15–240 min.

Received: January 28, 2013
Revised: March 28, 2013

Keywords: electrochemistry · porous silicon · reaction mechanisms · stain etching · surface chemistry

[1] a) V. Lehmann, *Electrochemistry of Silicon: Instrumentation, Science, Materials and Applications*, Wiley-VCH, Weinheim, **2002**; b) N. Koshida, T. Ohta, B. Gelloz, A. Kojima, *Curr. Opin. Solid State Mater. Sci.* **2011**, *15*, 183–187; c) Z. Huang, N. Geyer, P. Werner, J. de Boor, U. Gösele, *Adv. Mater.* **2011**, *23*, 285–308; d) G. E. Kotkovskiy, Y. A. Kuzishchin, I. L. Martynov, A. A. Chistyakov, I. Nabiev, *Phys. Chem. Chem. Phys.* **2012**, *14*, 13890–13902.

[2] J. Acker, A. Rietig, M. Steinert, V. Hoffmann, *J. Phys. Chem. C* **2012**, *116*, 20380–20388.

[3] K. W. Kolasinski, J. W. Gogola, W. B. Barclay, *J. Phys. Chem. C* **2012**, *116*, 21472–21481.

[4] A. Loni, D. Barwick, L. Batchelor, J. Tunbridge, Y. Han, Z. Y. Li, L. T. Canham, *Electrochem. Solid-State Lett.* **2011**, *14*, K25–K27.

[5] K. Sato, H. Tsuji, K. Hirakuri, N. Fukata, Y. Yamauchi, *Chem. Commun.* **2009**, 3759–3761.

[6] a) H. Gerischer, P. Allongue, V. Costa Kieling, *Ber. Bunsen-Ges.* **1993**, *97*, 753–756; b) K. W. Kolasinski, *Phys. Chem. Chem. Phys.* **2003**, *5*, 1270–1278; c) K. W. Kolasinski, *Surf. Sci.* **2009**, *603*, 1904–1911.

[7] a) D. R. Turner, *J. Electrochem. Soc.* **1960**, *107*, 810–816; b) J. J. Kelly, X. H. Xia, C. M. A. Ashruf, P. J. French, *IEEE Sens. J.* **2001**, *1*, 127–142.

[8] M. E. Dudley, K. W. Kolasinski, *Electrochem. Solid-State Lett.* **2009**, *12*, D22–D26.

[9] a) K. W. Kolasinski, J. Yadlovskiy, *Phys. Status Solidi C* **2011**, *8*, 1749–1753; b) K. W. Kolasinski, J. D. Hartline, B. T. Kelly, J. Yadlovskiy, *Mol. Phys.* **2010**, *108*, 1033–1043.

[10] K. W. Kolasinski, *J. Phys. Chem. C* **2010**, *114*, 22098–22105.

[11] a) E. Skúlason, V. Tripkovic, M. E. Björketun, S. Gudmundsdóttir, G. Karlberg, J. Rossmeisl, T. Bligaard, H. Jónsson, J. K. Nørskov, *J. Phys. Chem. C* **2010**, *114*, 18182–18197; b) E. Santos, P. Quaino, W. Schmickler, *Phys. Chem. Chem. Phys.* **2012**, *14*, 11224–11233.

[12] a) V. Schmidt, J. V. Wittemann, U. Gösele, *Chem. Rev.* **2010**, *110*, 361–388; b) K. Q. Peng, Y. Wu, H. Fang, X. Y. Zhong, Y. Xu, J. Zhu, *Angew. Chem.* **2005**, *117*, 2797–2802; *Angew. Chem. Int. Ed.* **2005**, *44*, 2737–2742; c) X. Wang, K. Q. Peng, X. J. Pan, X. Chen, Y. Yang, L. Li, X. M. Meng, W. J. Zhang, S. T. Lee, *Angew. Chem.* **2011**, *123*, 10035–10039; *Angew. Chem.* **2011**, *123*, 10035–10039; *Angew. Chem. Int. Ed.* **2011**, *50*, 9861–9865.

[13] K. W. Kolasinski, W. B. Barclay, *ECS Trans.* **2013**, *50*, in press.